

Convergence on the Proton Drip-Line in Thulium

B. Kootte,^{1,2,*} M.P. Reiter,^{2,3,4} C. Andreoiu,⁵ S. Beck,^{3,6} J. Bergmann,³ T. Brunner,⁷ T. Dickel,^{3,6} K.A. Dietrich,^{8,2} J. Dilling,^{9,10} E. Dunling,² J. Flowerdew,¹¹ L. Graham,² G. Gwinner,¹ Z. Hockenbery,^{7,2} C. Izzo,² A. Jacobs,^{12,2} A. Javaji,^{12,2} R. Klawitter,^{8,2} Y. Lan,^{12,2} E. Leistenschneider,^{12,2} E.M. Lykiardopoulou,^{12,2} I. Miskun,³ I. Mukul,² T. Murböck,² S.F. Paul,^{8,2} W.R. Plaß,^{3,6} J. Ringuette,^{13,2} C. Scheidenberger,^{3,6,14} R. Silwal,^{2,15} R. Simpson,^{2,12} A. Teigelhöfer,² R.I. Thompson,¹¹ J.L. Tracy, Jr.,² M. Vansteenkiste,² R. Weil,^{2,12} M.E. Wieser,¹¹ C. Will,³ and A.A. Kwiatkowski^{2,16}

¹*Department of Physics and Astronomy, University of Manitoba,
30A Sifton Road, Winnipeg, MB, R3T 2N2, Canada*

²*TRIUMF, 4004 Wesbrook Mall, Vancouver, BC, V6T 2A3, Canada*

³*II. Physikalisches Institut, Justus-Liebig-Universität, Heinrich-Buff-Ring 16, 35392 Gießen, Germany*

⁴*School of Physics and Astronomy, University of Edinburgh, James Clerk Maxwell Building,
Peter Guthrie Tait Road, Edinburgh EH9 3FD, Scotland, UK*

⁵*Department of Chemistry, Simon Fraser University,
8888 University Drive, Burnaby, BC, V5A 1S6, Canada*

⁶*GSI Helmholtzzentrum für Schwerionenforschung GmbH, Planckstraße 1, 64291 Darmstadt, Germany*

⁷*Physics Department, McGill University, 3600 rue University, Montréal, QC, H3A 2T8, Canada*

⁸*Fakultät für Physik und Astronomie, Ruprecht-Karls-Universität Heidelberg,
Im Neuenheimer Feld 226, 69120 Heidelberg, Germany*

⁹*Oak Ridge National Laboratory 1 Bethel Valley Road, Oak Ridge, TN, 37830, USA*

¹⁰*Physics Department, Duke University, 120 Science Drive, Campus Box 90305 Durham, NC, 27708, USA*

¹¹*Department of Physics and Astronomy, University of Calgary,
2500 University Drive NW, Calgary, AB, T2N 1N4, Canada*

¹²*Department of Physics and Astronomy, University of British Columbia,
6224 Agricultural Road, Vancouver, BC, V6T 1Z1, Canada*

¹³*Department of Physics, Colorado School of Mines, 1500 Illinois St., Golden, CO, 80401, USA*

¹⁴*Helmholtz Forschungsakademie Hessen für FAIR (HFHF),
GSI Helmholtzzentrum für Schwerionenforschung,
Campus Gießen, Heinrich-Buff-Ring 16, 35392 Gießen, Germany*

¹⁵*Department of Physics and Astronomy, Appalachian State University,
231 Garwood Hall, 525 Rivers Street, Boone, NC, 28608, USA*

¹⁶*Department of Physics and Astronomy, University of Victoria,
3800 Finnerty Road, Victoria, BC, V8P 5C2, Canada*

(Dated: July 10, 2025)

Direct observation of proton emission for very small Q -values is often unfeasible due to the long partial half-lives of the proton emission channel associated with tunneling through the Coulomb barrier. Therefore, proton emitters with very small decay energies may require the masses of both parent and daughter nuclei in order to establish them as proton unbound. Nuclear mass models have been used to predict the proton drip-line of the thulium (Tm) isotopic chain ($Z = 69$), but until now the proton separation energy has not been experimentally tested. Mass measurements were performed using a Multiple Reflection Time-Of-Flight Mass Spectrometer (MR-TOF-MS) at TRIUMF's TITAN facility to conclusively map the limit of proton-bound Tm. The masses of neutron-deficient, ^{149}Tm and ^{150}Tm , combined with measurements of $^{149m,g}\text{Er}$ (which were found to deviate from literature by ~ 150 keV), provide the first experimental confirmation that ^{149}Tm is the first proton-unbound nuclide in the Tm chain. Our measurements also enable the strength of the $N = 82$ neutron shell gap to be determined at the Tm proton drip-line, providing evidence supporting its continued existence.

I. INTRODUCTION

When isotopes become sufficiently neutron-deficient it eventually becomes energetically possible for one or more protons to spontaneously escape the nucleus. This transition within an isotopic chain to one or more protons being unbound is known as the *proton drip-line*, and its

location is of fundamental interest. It can be experimentally determined through measurements of the one-proton separation energy, S_p , and a nucleus is said to lie beyond the proton drip-line when $S_p \leq 0$ (i.e. it is *proton-unbound*) [1, 2]. Studying the location of the proton drip-line provides a valuable benchmark for the various nuclear models which predict the properties of unstable nuclei.

Near the proton drip-line, a proton must tunnel through the Coulomb barrier in order to be emitted (i.e. a single-nucleon analogue to α -decay). In contrast to

* Corresponding author (brian.a.kootte@jyu.fi)

alpha decay however, it is simpler to calculate the proton emission decay rate or spectroscopic factor, since the decay does not require the formation of a cluster of nucleons [1]. Proton emission is significantly influenced by the centrifugal barrier and the proton emission half-life at a given proton number, Z , depends strongly on underlying nuclear structure including the angular momentum carried away by the emitted proton [1][3][4], and the decay energy, Q_p [4].

Furthermore, the nuclear shell structure can change towards the drip-line; effects such as the weakening or disappearance of shells (quenching) at the classical magic numbers, and the appearance of new magic numbers have been both predicted and observed [5, 6]. Nuclear masses and binding energies provide indispensable information when studying the limits of nuclear existence and shell structure. They allow calculations of the particle separation energies and can be used to make predictions regarding the underlying nuclear structure and nuclear properties such as half-life, angular momentum, or spectroscopic factors in the case of proton emission.

The mass values of nuclides across the $N = 82$ shell closure, formed between the $h_{11/2}$ (or nearby $s_{1/2}$ or $d_{3/2}$) and the $f_{7/2}$ orbitals, have been intensively studied on the neutron-rich side of the nuclear chart, see e.g. [7–12]. Corresponding investigations at the neutron-deficient $N = 82$ shell closure up to the elements of holmium ($Z = 67$) and erbium ($Z = 68$) have been performed by ISOLTRAP [13], the ESR using Schottky Mass Spectrometry [14], and recently in ytterbium ($Z = 70$) at TITAN [15]. The proton drip-line around $Z = 69$ is associated with an abrupt change in the deformation [1, 16, 17]. Although masses of neutron-deficient thulium isotopes have been measured by SHIPTRAP [18], measurements remain elusive across the $N = 82$ shell closure where the one-proton drip-line is predicted to lie. The MR-TOF-MS technique [19] is well suited for measurements of short-lived isotopes. Here we report the first high-precision mass measurements of neutron-deficient thulium isotopes at the proton drip-line, enabling S_{2N} to be determined across $N = 82$.

A. Background

Ground state proton emission can occur for any nucleus beyond the proton drip-line, and was first observed in 1982 in ^{151}Lu and ^{147}Tm [20, 21]. Since then, at least 27 heavy ground state proton emitters have been identified, along with a number of isomeric states [22][23].

While ^{147}Tm has long been known to be a proton emitter, and prior direct mass measurements of ^{147}Tm and ^{148}Tm have been able to constrain the location of the proton drip-line to lie somewhere between $A = 148$ and $A = 151$ [18], the precise isotope at which Tm becomes proton-unbound remains uncertain due to the thus far unmeasured masses of ^{149}Tm and ^{150}Tm . In cases where neither observation of the decay nor direct mass mea-

surements can be used to establish the drip-line, various theoretical approaches are employed to predict its location, but these models are known to struggle to predict S_p far from stability [24].

Density functional theory and phenomenological descriptions of the nuclear binding energy have been utilized to predict the location of the proton drip-line. For instance, the Skyrme results of [25] can be used to interpolate the S_p of odd- Z nuclei. However, for ^{149}Tm , the choice of energy density functional – such as UNEDF1 [26] or SV-min [27] – leads to competing predictions regarding its position relative to the drip-line. Furthermore, the newer BSkG3 model [28] predicts the drip-line to be even closer to stability.

Bayesian model averaging can be used to assign weights to models in an attempt to improve estimates of the binding energies of heavy nuclei [29]. A recent Bayesian statistical analysis was performed to weight the proton drip-line predictions provided by several different energy density functionals, as well as FRDM2012 and HFB-24 [30]. This work predicted the last proton-bound isotope of Tm to occur at $N = 81$ ($A = 150$), but this has never been experimentally verified. The precise location of the thulium proton drip-line remains a significant gap in our experimental knowledge of the heavy, proton-deficient nuclei. The present measurement aims to determine the exact position of the ground state proton drip-line for Tm ($Z = 69$).

II. EXPERIMENTAL DESCRIPTION

The isotopes under study were produced throughout two experimental campaigns at TRIUMF’s Isotope Separator and Accelerator (ISAC) facility [31] using the ISOL (Isotope Separation On-Line) technique. A 480 MeV proton beam was impinged on a Ta target to produce rare isotopes via spallation reactions and the produced Tm and Er isotopes were surface ionized. The continuous beam of neutron-deficient isotopes was purified using the ISAC high-resolution mass separator [32] (resolving power ~ 2500) to select beams from $A = 149$ to $A = 157$ before preparation in the TITAN Radio-Frequency Quadrupole (RFQ) cooler-buncher trap [33] for precision mass measurements. The resulting bunches of ions were extracted and their kinetic energy matched for injection into TITAN’s MR-TOF-MS [34][35][36] to obtain a mass spectrum. Ions were again cooled and narrowly bunched in the injection trap of the MR-TOF-MS, before they underwent isochronous (energy independent) reflections between two electrostatic ion mirrors before time-of-flight detection using a MagneTOFTM ion detector manufactured by *ETP ion detect*. All ions observed in the spectrum were delivered and measured in a 1+ charge state and any possible non-isobars present due to charge exchange were removed using a *Mass Range Selector* [37, 38]. An example spectrum of $A = 149$ is given in Figure 1.

Measurements of the nuclei furthest from stability were made possible by employing so-called *mass selective re-trapping* [39, 40], during which the ion bunch is captured a second time in the injection trap after a first stage of mass separation in the MR-TOF-MS. Mass selective re-trapping can be used to selectively reduce the intensity of the dominant contaminant species by more than three orders of magnitude [15]. This improved the signal-to-background ratio of the $^{149,150}\text{Tm}$ measurements and allowed the MR-TOF-MS to accept a higher overall beam rate while keeping the total number of ions detected per mass measurement cycle within an acceptable range.

During the initial experiment (experiment #1), isotopes were produced using a high-power tantalum target which is equipped with greater heat dissipation, whereas the second experiment (experiment #2) utilized a low-power tantalum target, for which an improved and more homogeneous thermal profile is believed to have enhanced the release of Tm and Er. In both experiments the proton beam from TRIUMF’s main driver cyclotron was impinging on the Ta production targets with beam currents ranging from approximately 25 to 50 μA .

The mass of ^{150}Tm was measured along with the Yb masses [15] obtained in experiment #1, which additionally provided anchor masses for alpha decay chains [41]. The resolving power of $\sim 270,000$ in this experiment resulted in a proton separation energy of ^{150}Tm which was very close to zero, and no definitive conclusion could be drawn as to whether this nucleus is proton-bound. The Tm data-set was greatly improved during experiment #2 by performing additional measurements which extended data to ^{149}Tm , and improved on the initial experimental uncertainties. In particular, experiment #2 benefited from improvements that were made to the MR-TOF-MS system to achieve $\sim 400,000$ resolving power and lower systematic uncertainty.

A. Analysis Procedure

The analysis procedure followed the description in [42]. At all mass units, we utilized a high abundance peak to correct for time-dependent drifts in the Time of Flight (TOF) spectrum using in-house developed data acquisition software [35]. Subsequently, masses were determined by fitting the peaks in each spectrum using a *hyper-exponentially-modified Gaussian* (hyperEMG) lineshape [43] and the emgfit python library available at [44]. This procedure involves first fitting an isolated high-statistics peak with a multi-dimensional function to precisely determine the shape (i.e. functional form) of a single peak (the *shape calibrant*) and then using multiple copies of this shape to fit all peaks in the spectrum. Next, the masses of all peaks in the spectrum were calibrated against a single species with a well-established mass (the *mass calibrant*). Appropriate shape and mass calibrant peaks were chosen for each set of isobars measured to minimize the influence of overlapping isobars and nuclear

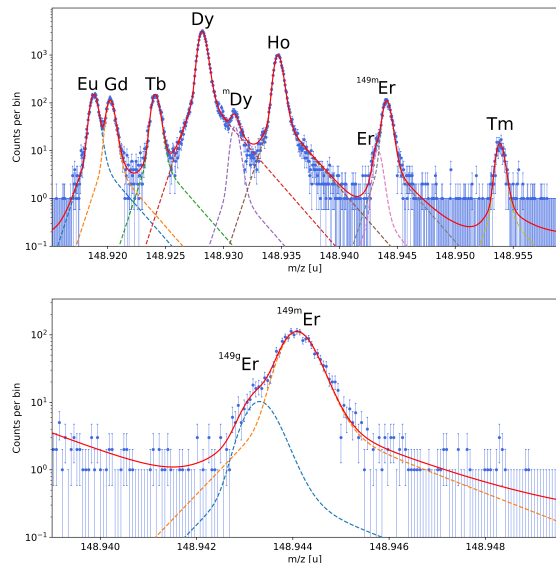


FIG. 1. Top: The $A = 149$ spectrum with major peaks labeled. ^{149}Dy is used as both shape and mass calibrant here (m indicates a long-lived isomer). Bottom: A fit of the $^{149g+m}\text{Er}$ peak using the hyperEMG functional form and calibrated to the shape of the higher statistics ^{149}Dy peak. The known peak shape enabled the mass of the ground state to be directly determined alongside the isomer within the mixed peak.

isomers. In the present analysis, the peaks corresponding to ^{149}Dy , ^{150}Ho , ^{151}Ho , ^{152}Dy , ^{153}Dy , ^{154}Dy , ^{155}Yb , ^{156}Yb , and ^{157}Yb were selected as shape calibrants in their respective isobaric mass spectra. The chosen mass calibrant at each mass number was cross-checked for consistency with the masses of several different isobars listed in the 2020 Atomic Mass Evaluation (AME2020) to confirm its identity, and are listed in Table I.

B. Results

In this work, mass measurements across 17 neutron-deficient Tm and Er isotopes were obtained, with ^{149}Tm , ^{150}Tm representing first-time measurements. Mass excess values are defined as the sum of the ionic mass and the electron mass (since all ions were singly-charged) minus the mass number A .

The final mass values were obtained by adding the experimental and known systematic uncertainties in quadrature and making corrections for any known or expected unresolved isomers. These are summarized in Table I. Additionally, Table II contains the uncorrected measurement data – excluding any isomer corrections – and is provided as a reference should new information about these isomers become available in the future. Mass excess (ME) uncertainties include the uncertainty of the calibrant mass, while the Ion Mass Ratio uncertainties do not. The systematic uncertainty was dominated by nonideal switching of voltages in the ion mirror on the

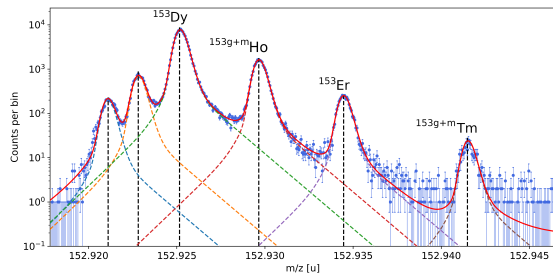


FIG. 2. Fit of the overlapping peaks in the $A = 153$ spectrum with a hyperEMG functional form.

extraction side, and was measured using stable ions as described in [45] and [42]. The single measurement presented here from experiment #1, ^{150}Tm , includes a systematic uncertainty of 3×10^{-7} , while the measurements obtained during experiment #2 incorporate a systematic uncertainty of 1.5×10^{-7} (except $A=153$). This reduction was the result of improvements made to the tune of the MR-TOF-MS and the stability of the high-voltage electrodes.

The crowded $A = 153$ spectrum shown in Figure 2 was the most challenging from which to obtain a high-statistics shape calibrant in the analysis. An isobaric species lies in each of the two tails of the ^{153}Dy shape/mass calibrant, and the functional form needed to be manually selected in order to ignore excessive influence on the fitting algorithm from the isobar in the lower mass tail. Furthermore, the mass 153 spectrum had a total rate of ~ 3.8 ions per trapping cycle, with ~ 2.7 per cycle in the ^{153}Dy calibrant peak. Therefore, an additional systematic uncertainty of 8×10^{-8} per ion per cycle (3×10^{-7} total) was required to account for ion-ion interactions (based on off-line tests).

According to ENSDF, ^{153}Tm has a long-lived isomer at 43.2 ± 0.2 keV [46] and ^{155}Tm one at 41 ± 6 keV [47]. ^{151}Tm , ^{152}Tm , and ^{154}Tm respectively contain a ~ 7 s, a 5.2 s, and a 3.3 s isomer [48–50] for which the excitation energy was taken from NUBASE 2020 [51] to be 93 ± 6 keV, -100 ± 250 keV, and 70 ± 50 keV. NUBASE 2020 also infers excitation energies for ^{149}Tm ($100\# \pm 50\#$ keV) [52] and ^{150}Tm ($140\# \pm 140\#$ keV) [53] from trends in neighbouring nuclei; the higher 671 keV, 5.2 ms isomer of ^{150}Tm is not expected to be observable in this experiment due to its short half-life and no indication of it was observed. ^{157}Lu also contains an unknown contribution from a 20.9 ± 2.0 keV isomer (4.8 s) [54].

Since these isomeric contributions may shift the determined mass to appear heavier than for a peak containing only the ground state, the standard procedure outlined in Appendix B of AME2020 [55] was used to determine an appropriate correction to the mass and the corresponding increase in uncertainty. The ground state mass (m_{gs}) was obtained from the experimental mass (m_{exp}) and the previously reported excitation energy (ΔE) through the relation $m_{gs} = m_{exp} - \Delta E/2$, and additional uncertain-

ties of $0.290(\Delta E)$, and $\frac{1}{2}\sigma_1$ were added in quadrature with the experimental error, where σ_1 is the uncertainty in the reported excitation energy. The Mass Excesses and Ion Mass Ratio was thus corrected for all species likely containing an unresolved isomer (e.g. 13 keV for ^{153g}Tm and 12 keV for ^{155g}Tm).

The mass spectra of $^{149,150}\text{Tm}$ strongly benefited from using mass selective re-trapping to improve the Tm-to-contaminant ratio by about three to four orders of magnitude depending on their separation, as shown in Figure 1 of reference [15]. Once applied, the peaks were observable above the background and could be fit.

As seen in Figure 3, our measured mass values show overall agreement with the literature values from AME2020, including for ^{157}Tm and ^{156}Tm which are not known to have long-lived isomers or isobaric species that could impact our measurements. The two new mass values of $^{149,150}\text{Tm}$ now close a gap in the long chain of previously measured neutron-deficient isotopes of Tm [18, 56, 57], with mass data now spanning from the proton emitter ^{147}Tm at $N=78$ to stable ^{169}Tm at $N=100$. Alongside the measured Tm isotopes, $^{149-154}\text{Er}$ were also identified in the mass spectra. The masses of $^{150-154}\text{Er}$ all lie within 1.5σ of the presently accepted values in the AME2020 and any known isomers are > 2.5 MeV above the ground state and thus do not impact the measurements. After correcting for the isomer, our measurement of ^{157}Lu yields a mass 56 ± 29 keV heavier than the AME value.

^{149g}Er and ^{149m}Er (bottom Figure 1) were fit using two hyperEMG functions calibrated to the shape of the ^{149}Dy peak. The known $11/2^-$ isomeric state was delivered to TITAN at greater intensity and the ground state peak shows up as an excess in the left shoulder. Our ^{149g}Er and ^{149m}Er masses were found to be heavier by 2.9σ and 3.9σ respectively when compared to the literature value obtained via a measurement of ^{149m}Er at the GSI ESR [14]. This results in a shift of the S_p of ^{150}Tm (see below).

III. DISCUSSION

As detailed below, our measurements of the Tm and Er mass chains establish ^{149}Tm as the first proton-unbound Tm isotope. Furthermore, they support recent evidence for the persistence of the shell closure at $Z = 70$ [15] with a corresponding measurement of the trend in Δ_2N at $Z = 69$.

Last Proton-Bound Isotope Determined from $^{149m,149g}\text{Er}$ and ^{150g}Tm

The Er isotopic chain was measured alongside Tm during experiment #2 from ^{154}Er to ^{149}Er . During this second measurement, a discrepancy in the mass of ^{149g}Er relative to the literature value was found which signifi-

TABLE I. List of isotopes, their respective calibrants (AME2020 values), measured ion mass ratios, and the mass excesses when referenced to the AME2020 values of the calibrant (uncertainty added in quadrature). The ^{150}Tm mass from experiment #1 [15] is included at the bottom. The # indicates an extrapolated mass in the AME2020. Nuclides with a * have a long-lived isomer for which the excitation energy is reported in NUBASE and relies on alpha decay data, and nuclides with a ** rely on extrapolations. Nuclides with a † contained an unresolved admixture of the ground state and an isomer in the peak for which the known excitation energy is listed in both ENSDF and NUBASE. The mass excess and the ion mass ratio of any peaks likely to contain an unresolved isomeric contribution were corrected by $0.5 \times$ the listed excitation energy (listed in **bold**) and a corresponding additional uncertainty was incorporated (see Section III). The ^{155}Tm peak has an unresolved 41(6)keV isomer [47], ^{153}Tm has a 43.2 ± 0.2 keV isomer [46], and ^{157}Lu has a 20.9 ± 2.0 keV isomer [54]. As described in the text, these values were corrected using the procedure outlined in the 2020 Atomic Mass Evaluation (AME2020) [55] to obtain a mass for the ground state and its uncertainty. The difference between the TITAN measurement and the AME2020 value is given with the AME and the measurement uncertainty added in quadrature.

| Species | Calibrant | Ion Mass Ratio | ME _{Measured} (keV) | ME _{AME2020} (keV) | TITAN - AME (keV) |
|------------------------------|-------------------|-----------------------|------------------------------|-----------------------------|-------------------|
| ^{157g}Lu † | ^{157}Yb | 1.00004813(16) | -46384 (26) | -46440 (12) | 56(29) |
| ^{157}Tm | ^{157}Yb | 0.99996379(18) | -58714 (28) | -58709 (28) | -4(40) |
| ^{156}Tm | ^{156}Yb | 0.99997554(15) | -56818 (24) | -56834 (14) | 17(28) |
| ^{155g}Tm † | ^{155}Er | 1.00003875(17) | -56617 (26) | -56626 (10) | 9(28) |
| ^{155}Yb | ^{155}Er | 1.00008157(15) | -50437 (23) | -50503 (17) | 66(28) |
| ^{154g}Tm * | ^{154}Dy | 1.00011154(29) | -54401 (42) | -54427 (14) | 26(44) |
| ^{154}Er | ^{154}Dy | 1.00005458(16) | -62569 (24) | -62605 (5) | 36(24) |
| ^{153g}Tm † | ^{153}Dy | 1.00010661(37) | -53957 (54) | -53973 (12) | 16(55) |
| ^{153}Er | ^{153}Dy | 1.00006064(34) | -60505 (48) | -60467 (9) | -39(49) |
| ^{152g}Tm * | ^{152}Dy | 1.00013131(94) | -51535 (133) | -51720 (50) | 186(142) |
| ^{152}Er | ^{152}Dy | 1.00006789(18) | -60510 (26) | -60500 (9) | -10(27) |
| ^{151g}Tm * | ^{151}Dy | 1.00012788(26) | -50774 (36) | -50772 (19) | -3(41) |
| ^{151}Er | ^{151}Dy | 1.00007472(15) | -58248 (22) | -58266 (16) | 19(27) |
| ^{150g}Tm ** | ^{150}Dy | 1.00016335(62) | -46497 (87) | -46490 (200#) | ## |
| ^{150}Er | ^{150}Dy | 1.00008237(16) | -57807 (23) | -57831 (17) | 24(29) |
| ^{149g}Tm ** | ^{149}Dy | 1.00017215(36) | -43812 (51) | -43940 (200#) | ## |
| ^{149g}Er | ^{149}Dy | 1.00010171(33) | -53584 (47) | -53742 (28) | 158(55) |
| ^{149m}Er | ^{149}Dy | 1.00010695(16) | -52857 (25) | -53000 (28) | 143(37) |
| ^{150g}Tm (Exp 1)** | ^{150}Dy | 1.00016357(73) | -46467 (103) | -46490 (200#) | ## |

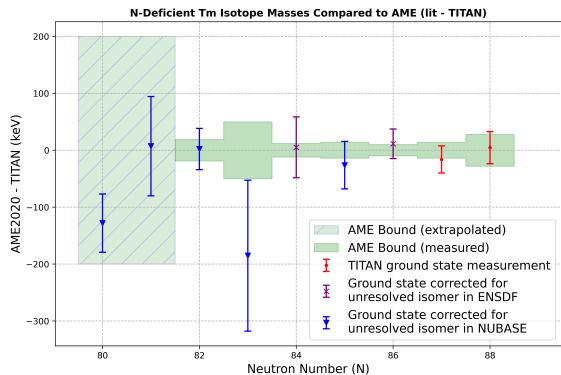


FIG. 3. Comparison of the measured Tm isotopes with the error bounds on the ground state given in the 2020 Atomic Mass Evaluation. The masses and error bars of measurements marked with a purple “x” or a blue triangle were corrected for unresolved long-lived isomers listed in ENSDF and NUBASE respectively.

cantly affects the one-proton separation energy (S_p) of the ^{150}Tm ground state. Together, the newly-measured ^{150}Tm mass and the AME2020 mass of ^{149g}Er results in a S_p that is well within 1σ of zero, but using both up-

dated masses yields a positive proton separation energy consistent with proton-bound ^{150}Tm (2σ).

As with ^{151}Yb , for which the ISAC target was seen to preferentially deliver the spin 11/2 isomer over the ground state, ^{149}Er , having two fewer protons, similarly appeared to favour the excited state. We therefore fit the two-component ^{149}Er peak using two hyperEMG functions having the same parameters as the ^{149}Dy peak; this yields mass values for both the dominant isomeric state ($t_{1/2} = 8.9 \pm 0.2$ s), as well as the ground state ($t_{1/2} = 4 \pm 2$ s) which shows up as an excess within the low-mass tail of the isomer peak.

The ground state mass of ^{149}Er can be determined by two different methods using our data. One approach is to extract it from the measured isomer mass and the known excitation energy as was previously done in an experiment using Schottky mass spectrometry [14], which reported an uncertainty of ± 28 keV. The other method is to obtain the mass directly from the fit of the ground state within the tail of the isomer using the known peak shape.

The first approach obtains the mass of ^{149g}Er using the known isomeric excitation energy which was initially measured via a two γ -ray internal transition to the ground state proceeding through a 630.5 keV (M4) \rightarrow

111.0 keV (M1) cascade [58] This was later confirmed in subsequent experiments which yielded 630.3 keV \rightarrow 111.3 keV [59] and 630.5 \pm 2.6 keV \rightarrow 111.3 \pm 1.1 keV by [60]. The ^{149m}Er isomer is established to lie 741.8 \pm 0.2 keV above the ground state according to the NUBASE 2020 evaluation [51].

This excitation energy is consistent with our recent result in which the newly measured masses of $^{151g+m}\text{Yb}$ were used to support a theoretical explanation for the remarkably consistent first excitation energy (approximately 750 keV) in the isotonic chain containing ^{149}Er [15]. This has been attributed to a clustering of single-proton energy levels for the mildly deformed nuclei at $N = 81$ [15] resulting from the single hole in the $h_{11/2}$ neutron orbital common to ^{149}Er and many of its isotones [58]. This provides increased confidence in the reliability of the established excitation energy of the long-lived 741.69 \pm 0.23 keV isomer ^{149m}Er (9.6 \pm 0.6 s). Using this value with our current mass measurement of ^{149m}Er to indirectly determine the ground state mass yields a ^{149g}Er mass excess of -53599 \pm 25 keV, a 143 keV increase from AME2020.

However, the present dataset also enables a more direct measurement of the ground state mass by utilizing the lower abundance, overlapping TOF peak of the ground state of ^{149}Er and employing a hyperEMG fitting procedure. Directly fitting the lower abundance ^{149g}Er (as in Figure 1) with the hyperEMG function calibrated to the shape of the ^{149}Dy peak yields a mass excess of -53584 \pm 47 keV, an increase in mass of 158 \pm 55 keV from the AME2020 value. The excitation energy of ^{149m}Er can then be determined from the difference between our measurements of ground state and isomer to be 726 \pm 53 keV.

While the newly determined mass of ^{149g}Er and the isomer ^{149m}Er deviate from the mass value in the AME2020, they are consistent with observable trends in the binding energy of nuclides in this region. The cause of our discrepancy in our measurement of this single mass is unknown, but may warrant a third measurement of the $^{149g,m}\text{Er}$ isotope for confirmation.

These new masses of the ^{149}Er isomer and ground state lead us to adopt a revised one-proton separation energy of the ground state which directly impacts the location of the proton drip-line in Tm, since the proton separation energy of a nucleus depends on both the mass of the candidate proton emitter as well as on the mass of the daughter nucleus of the decay. Both the $^{149,150}\text{Tm}$ masses as well as the revised ^{149}Er value were thus needed for an unambiguous identification of the Tm drip-line, since the new Tm masses alone did not exclude the possibility that ^{150}Tm could also be proton-unbound when using the ^{149}Er value from the AME2020. These measurements confirm that ^{150}Tm is indeed proton-bound, agreeing qualitatively with the *Bayesian model averaging* predictions of [30] that ^{149}Tm is the first proton-unbound thulium isotope. Furthermore, the proton emission Q-value of ^{149}Tm has been determined and can now be used as an input for decay rate calculations.

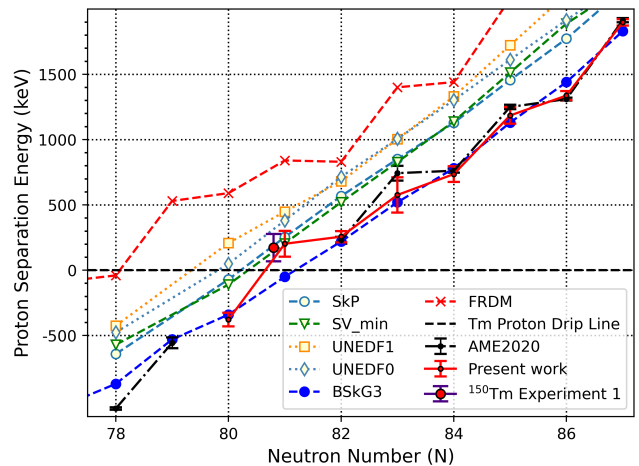


FIG. 4. The one-proton separation energy (S_p) of Tm isotopes calculated from the present measurements of masses in the Tm ($Z = 69$) and Er ($Z = 68$) isotopic chains is shown in red and connected by solid lines (The ^{150}Tm data point from experiment #1 is offset horizontally for clarity). This includes our new mass of ^{149}Er at $N = 81$, but masses from the 2020 AME [61] were used for ^1H , ^{148}Er ($N = 80$), and ^{155}Er ($N = 87$) in calculating S_p for Tm. Theoretical calculations of S_p are shown for comparison. Corrections were made for measurements possibly containing unresolved, long-lived, isomeric states (including the extrapolated isomers in $^{149,150}\text{Tm}$) but do not impact the conclusion that ^{150}Tm is the last proton-bound Tm isotope.

^{149}Tm : The First p-Unbound Isotope

The proton emission energy can be determined from $Q = -S_p = M(Z, N) - M(Z - 1, N) - M(^1\text{H})$. Our direct measurements of ^{149g}Er and ^{150g}Tm show ^{150g}Tm to be proton-bound, having a Q-value of -202 \pm 99 keV. Meanwhile, our measurement of ^{149g}Tm establishes it as the first proton-unbound isotope in the thulium chain. For it we obtain a proton emission Q-value of +378 \pm 52 keV when calculated using the measured mass of ^{149g}Tm and the masses of ^{148}Er and ^1H from the AME2020. This decay energy is on the high side of the AME extrapolation of 250 \pm 201 keV and can be used in estimations of the proton emission half-life for a given angular momentum transfer (e.g. [3, 4]). The small Q-value of the ^{149g}Tm decay allows for it to proceed to only one possible final state, the 0+ ground state of ^{148}Er , so it is expected that $J^\pi = 11/2^-$. Both of the above decay Q-values and their uncertainties take into account the expected unresolved isomers listed in NUBASE inferred from trends in neighbouring nuclei.

Aside from BSkG3 [28], the models in Figure 4 systematically over-predict S_p . Thus the present measurements demonstrate that ^{149}Tm is the first proton-unbound nucleus, rather than ^{148}Tm or ^{150}Tm .

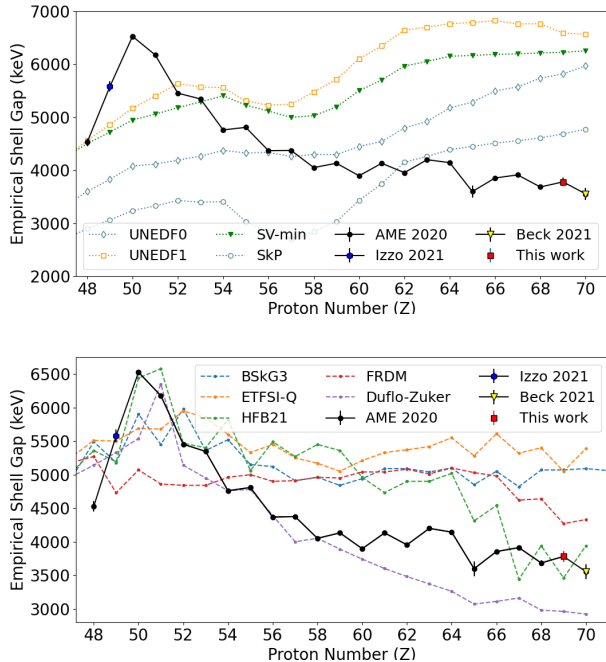


FIG. 5. Comparison of models and experimental data for the empirical shell gap (Δ_{2N}) split into two figures for clarity. The mass data from [68] and [15] was added for $Z = 49$ and $Z = 70$ respectively. A selection of Density Functional Theory and “liquid drop” models are shown.

Evolution of the $N = 82$ Neutron Shell Closure

In addition to determining the location of the drip-line, the new masses of $^{149/150}\text{Tm}$ allow for a comparison to predictions of the empirical shell gap of the $N = 82$ shell closure defined by $\Delta_{2N} = ME(N, Z + 2) + ME(N, Z - 2) - 2ME(N, Z)$ (see Figure 5). The models shown include UNEDF0 [62], UNEDF1 [26], HFB21 [63], Duflo-Zucker [64], FRDM [65], SkP [66], SV-min [27], and ETFSI-Q [67]. In this region most models over-predict the shell gap of the $N=82$ isotone chain by 0.5-3 MeV with the exceptions of Duflo-Zucker under-predicting by nearly 1 MeV and HFB21 which lies within 500 keV of the isotones from $Z = 67$ to 70.

The present work measures the Δ_{2N} of Tm at the $N=82$ shell closure and shows that it is, in fact, the first isotone for which Δ_{2N} depends on the binding energy of a proton-unbound nucleus (^{149}Tm). These measurements indicate the persistence of the $N = 82$ shell closure, which is consistent with the recent corresponding measurement of Yb [15]. Furthermore, the empirical shell gap at $Z=69$ continues the trend seen in the more stable $N = 82$ nuclei such as $Z=63$ and 67 of having a local maximum in Δ_{2N} at the odd- Z nuclei.

IV. CONCLUSION AND OUTLOOK

The masses of neutron deficient Tm and Er isotopes obtained in this work identify the precise location of the proton drip-line in the Tm isotopic chain. The transition from positive to negative proton separation energy is observed between ^{149g}Tm and ^{150g}Tm . Our updated mass of ^{149}Er directly impacts the proton-bound nature of ^{150}Tm since it would be the daughter nucleus of the proton emission if this decay mode were possible. The masses of two previously unmeasured Tm isotopes were measured in this experiment. Additionally, an update to the previously measured mass of ^{149m}Er and a first direct measurement of the ground state ^{149g}Er determined them to be ~ 150 keV heavier than the current literature values, thereby establishing ^{150g}Tm as proton-bound.

The well-understood composition of the mass spectra provides confidence in our identification of isotopes using the MR-TOF-MS. The mass of ^{149g}Er was determined directly by performing hyperEMG fits on the time-of-flight spectrum obtained with TITAN’s MR-TOF-MS and indirectly through the ^{149m}Er isomer. Together, our masses of ^{149g}Tm , ^{150g}Tm , and ^{149g}Er establish that ^{149g}Tm , having 20 fewer neutrons than the only stable isotope of Tm (^{169}Tm , $N = 100$), is the first proton-unbound ground state in this isotopic chain. This agrees with the drip-line prediction obtained from a recent Bayesian analysis of various theoretical models [30].

Our update to the literature masses also highlights the importance of measuring and reporting not only the masses of previously unmeasured isotopes but also confirmations of literature mass values which provide input for various models and predictions. Heavier exotic species pose challenges that arise from the abundance of isomers and isobaric molecules that must be identified and, therefore, must be treated with caution. The mass values presented here provide a new benchmark for the models used to predict the binding energies of unmeasured nuclei in the neutron-deficient region near $N=82$ and establish the $Z=69$ proton drip-line.

V. ACKNOWLEDGEMENTS

TITAN is funded by the Natural Sciences and Engineering Research Council (NSERC) of Canada and through TRIUMF by the National Research Council (NRC) of Canada.

This work was further supported by the German Research Foundation (DFG), Grant No. 422761894; by the German Federal Ministry for Education and Research (BMBF), Grants No. 05P16RGFN1 and No. 05P19RGFN1; by the Hessian Ministry for Science and Art through the LOEWE Center HIC for FAIR; by the JLU and GSI Helmholtzzentrum für Schwerionenforschung under the JLU-GSI strategic Helmholtz partnership agreement.

For the purpose of open access, the authors have ap-

plied a creative commons attribution (CC BY) licence to any author accepted manuscript version arising.

-
- [1] P. J. Woods, C. N. Davids, *Nuclei Beyond The Proton Drip-Line*, *Annual Review of Nuclear and Particle Science* 47 (1) (1997) 541–590.
- [2] M. Pfützner, M. Karny, L. V. Grigorenko, K. Riisager, *Radioactive decays at limits of nuclear stability*, *Rev. Mod. Phys.* 84 (2) (2012) 567–619.
- [3] D. S. Delion, R. J. Liotta, R. Wyss, *Systematics of Proton Emission*, *Phys. Rev. Lett.* 96 (2006) 072501. doi:10.1103/PhysRevLett.96.072501. URL <https://link.aps.org/doi/10.1103/PhysRevLett.96.072501>
- [4] Z.-X. Zhang, J.-M. Dong, *A Formula for Half-life of Proton Radioactivity*, *Chin. Phys. C* 42 (1) (2018) 014104. doi:10.1088/1674-1137/42/1/014104. URL <https://doi.org/10.1088/1674-1137/42/1/014104>
- [5] O. Sorlin, M.-G. Porquet, *Nuclear magic numbers: New features far from stability*, *Progress in Particle and Nuclear Physics* 61 (2) (2008) 602–673. doi:<https://doi.org/10.1016/j.pnpnp.2008.05.001>. URL <https://www.sciencedirect.com/science/article/pii/S0146641008000380>
- [6] R. Kanungo, *A new view of nuclear shells*, *Physica Scripta* 2013 (T152) (2013) 014002. doi:10.1088/0031-8949/2013/T152/014002. URL <https://dx.doi.org/10.1088/0031-8949/2013/T152/014002>
- [7] M. Dworschak, G. Audi, K. Blaum, P. Delahaye, S. George, U. Hager, F. Herfurth, A. Herlert, A. Kellerbauer, H.-J. Kluge, et al., *Restoration of the N= 82 Shell Gap from Direct Mass Measurements of Sn 132, 134*, *Physical review letters* 100 (7) (2008) 072501.
- [8] M. Breitenfeldt, C. Borgmann, G. Audi, S. Baruah, D. Beck, K. Blaum, C. Böhm, R. B. Cakirli, R. Casten, P. Delahaye, et al., *Approaching the n= 82 shell closure with mass measurements of ag and cd isotopes*, *Physical Review C—Nuclear Physics* 81 (3) (2010) 034313.
- [9] D. Atanasov, P. Ascher, K. Blaum, R. B. Cakirli, T. E. Cocolios, S. George, S. Goriely, F. Herfurth, H.-T. Janka, O. Just, M. Kowalska, S. Kreim, D. Kisler, Y. A. Litvinov, D. Lunney, V. Manea, D. Neidherr, M. Rosenbusch, L. Schweikhard, A. Welker, F. Wienholtz, R. N. Wolf, K. Zuber, *Precision mass measurements of $^{129-131}\text{Cd}$ and their impact on stellar nucleosynthesis via the rapid neutron capture process*, *Phys. Rev. Lett.* 115 (2015) 232501. doi:10.1103/PhysRevLett.115.232501. URL <https://link.aps.org/doi/10.1103/PhysRevLett.115.232501>
- [10] R. Knöbel, M. Diwisch, F. Bosch, D. Boutin, L. Chen, C. Dimopoulou, A. Dolinskii, B. Franczak, B. Franzke, H. Geissel, et al., *First Direct Mass Measurements of Stored Neutron-rich $^{129,130,131}\text{Cd}$ Isotopes with FRS-ESR*, *Physics Letters B* 754 (2016) 288–293.
- [11] C. Babcock, R. Klawitter, E. Leistenschneider, D. Lascar, B. R. Barquest, A. Finlay, M. Foster, A. T. Gallant, P. Hunt, B. Kootte, Y. Lan, S. F. Paul, M. L. Phan, M. P. Reiter, B. Schultz, D. Short, C. Andreoiu, M. Brodeur, I. Dillmann, G. Gwinner, A. A. Kwiatkowski, K. G. Leach, J. Dilling, *Mass Measurements of Neutron-Rich Indium Isotopes Toward the $N = 82$ Shell Closure*, *Phys. Rev. C* 97 (2018) 024312. doi:10.1103/PhysRevC.97.024312. URL <https://link.aps.org/doi/10.1103/PhysRevC.97.024312>
- [12] V. Manea, J. Karthein, D. Atanasov, M. Bender, K. Blaum, T. E. Cocolios, S. Eliseev, A. Herlert, J. D. Holt, W. J. Huang, Y. A. Litvinov, D. Lunney, J. Menéndez, M. Mougeot, D. Neidherr, L. Schweikhard, A. Schwenk, J. Simonis, A. Welker, F. Wienholtz, K. Zuber, *First glimpse of the $n = 82$ shell closure below $z = 50$ from masses of neutron-rich cadmium isotopes and isomers*, *Phys. Rev. Lett.* 124 (2020) 092502. doi:10.1103/PhysRevLett.124.092502. URL <https://link.aps.org/doi/10.1103/PhysRevLett.124.092502>
- [13] D. Beck, F. Ames, G. Audi, G. Bollen, F. Herfurth, H. J. Kluge, A. Kohl, M. König, D. Lunney, I. Martel, et al., *Accurate Masses of Unstable Rare-earth Isotopes by ISOLTRAP*, *The European Physical Journal A* 8 (2000) 307–329.
- [14] Y. A. Litvinov, H. Geissel, T. Radon, F. Attallah, G. Audi, K. Beckert, F. Bosch, M. Falch, B. Franzke, M. Hausmann, et al., *Mass Measurement of Cooled Neutron-Deficient Bismuth Projectile Fragments with Time-Resolved Schottky Mass Spectrometry at the FRS-ESR Facility*, *Nuclear Physics A* 756 (1-2) (2005) 3–38.
- [15] S. Beck, B. Kootte, I. Dedes, T. Dickel, A. A. Kwiatkowski, E. M. Lykiardopoulou, W. R. Plaß, M. P. Reiter, C. Andreoiu, J. Bergmann, T. Brunner, D. Curien, J. Dilling, J. Dudek, E. Dunling, J. Flowerdew, A. Gaamouci, L. Graham, G. Gwinner, A. Jacobs, R. Klawitter, Y. Lan, E. Leistenschneider, N. Minkov, V. Monier, I. Mukul, S. F. Paul, C. Scheidenberger, R. I. Thompson, J. L. Tracy, M. Vansteenkiste, H.-L. Wang, M. E. Wieser, C. Will, J. Yang, *Mass Measurements of Neutron-Deficient Yb Isotopes and Nuclear Structure at the Extreme Proton-Rich Side of the N=82 Shell*, *Physical review letters* 127 (11) (2021) 112501–112501.
- [16] D. Delion, A. Dumitrescu, *Universal Proton Emission Systematics*, *Physical Review C* 103 (5) (2021) 054325.
- [17] L. Geng, H. Toki, J. Meng, *Proton-rich nuclei at and beyond the proton drip line in the relativistic mean field theory*, *Progress of theoretical physics* 112 (4) (2004) 603–617.
- [18] C. Rauth, D. Ackermann, K. Blaum, M. Block, A. Chaudhuri, Z. Di, S. Eliseev, R. Ferrer, D. Habs, F. Herfurth, F. P. Heßberger, S. Hofmann, H.-J. Kluge, G. Maero, A. Martín, G. Marx, M. Mukherjee, J. B. Neumayr, W. R. Plaß, S. Rahaman, D. Rodríguez, C. Scheidenberger, L. Schweikhard, P. G. Thirof, G. Vorobjev, C. Weber, *First Penning Trap Mass Measurements beyond the Proton Drip Line*, *Phys. Rev. Lett.* 100 (2008) 012501. doi:10.1103/PhysRevLett.100.012501. URL <https://link.aps.org/doi/10.1103/PhysRevLett.100.012501>

TABLE II. Data from Table I without correction for unresolved isomers. Nuclides with a * are known or expected to have a long-lived isomer that could not be resolved in this experiment. No correction is made here and no additional uncertainty added to account for the admixture.

| Species | Calibrant | Ion Mass Ratio | ME _{Measured} (keV) | ME _{AME2020} (keV) |
|-----------------------------|-------------------|----------------|------------------------------|-----------------------------|
| ^{157g+m} Lu | ¹⁵⁷ Yb | 1.00004820(16) | -46373 (25) | -46440 (12) |
| ¹⁵⁷ Tm | ¹⁵⁷ Yb | 0.99996379(18) | -58714 (28) | -58709 (28) |
| ¹⁵⁶ Tm | ¹⁵⁶ Yb | 0.99997554(15) | -56818 (24) | -56834 (14) |
| ^{155g+m} Tm * | ¹⁵⁵ Er | 1.00003889(15) | -56596 (23) | -56626 (10) |
| ¹⁵⁵ Yb | ¹⁵⁵ Er | 1.00008157(15) | -50437 (23) | -50503 (17) |
| ^{154g+m} Tm * | ¹⁵⁴ Dy | 1.00011179(18) | -54366 (26) | -54427 (14) |
| ¹⁵⁴ Er | ¹⁵⁴ Dy | 1.00005458(16) | -62569 (24) | -62605 (5) |
| ^{153g+m} Tm * | ¹⁵³ Dy | 1.00010676(36) | -53935 (52) | -53973 (12) |
| ¹⁵³ Er | ¹⁵³ Dy | 1.00006064(34) | -60505 (48) | -60467 (9) |
| ^{152g+m} Tm * | ¹⁵² Dy | 1.00013096(23) | -51585 (33) | -51720 (50) |
| ¹⁵² Er | ¹⁵² Dy | 1.00006789(18) | -60510 (26) | -60500 (9) |
| ^{151g+m} Tm * | ¹⁵¹ Dy | 1.00012821(17) | -50728 (24) | -50772 (19) |
| ¹⁵¹ Er | ¹⁵¹ Dy | 1.00007472(15) | -58248 (22) | -58266 (16) |
| ¹⁵⁰ Tm * | ¹⁵⁰ Dy | 1.00016386(23) | -46427 (33) | -46490 (200#) |
| ¹⁵⁰ Er | ¹⁵⁰ Dy | 1.00008237(16) | -57807 (23) | -57831 (17) |
| ¹⁴⁹ Tm * | ¹⁴⁹ Dy | 1.00017251(24) | -43762 (34) | -43940 (200#) |
| ^{149g} Er | ¹⁴⁹ Dy | 1.00010171(33) | -53584 (47) | -53742 (28) |
| ^{149m} Er | ¹⁴⁹ Dy | 1.00010695(17) | -52857 (25) | -53000 (28) |
| ¹⁵⁰ Tm (Exp 1) * | ¹⁵⁰ Dy | 1.00016407(45) | -46397 (63) | -46490 (200#) |

PhysRevLett.100.012501

- [19] H. Wollnik, M. Przewloka, Time-of-flight mass spectrometers with multiply reflected ion trajectories, International Journal of Mass Spectrometry and Ion Processes 96 (3) (1990) 267–274. doi:[https://doi.org/10.1016/0168-1176\(90\)85127-N](https://doi.org/10.1016/0168-1176(90)85127-N). URL <https://www.sciencedirect.com/science/article/pii/016811769085127N>
- [20] S. Hofmann, W. Reisdorf, G. Münzenberg, F. Heßberger, J. Schneider, P. Armbruster, Proton radioactivity of ¹⁵¹Lu, Zeitschrift für Physik A Atoms and Nuclei 305 (2) (1982) 111–123.
- [21] O. Klepper, T. Batsch, S. Hofmann, R. Kirchner, W. Kurcewicz, W. Reisdorf, E. Roeckl, D. Scharadt, G. Nyman, Direct and beta-delayed proton decay of very neutron-deficient rare-earth isotopes produced in the reaction ⁵⁸Ni + ⁹²Mo, Zeitschrift für Physik A Atoms and Nuclei 305 (2) (1982) 125–130.
- [22] B. Blank, M. Borge, Nuclear structure at the proton drip line: Advances with nuclear decay studies, Progress in Particle and Nuclear Physics 60 (2) (2008) 403–483. doi:<https://doi.org/10.1016/j.ppnp.2007.12.001>. URL <https://www.sciencedirect.com/science/article/pii/S0146641007000956>
- [23] Evaluated Nuclear Structure Data Files of Brookhaven National Laboratory (2021). URL <http://www.nndc.bnl.gov/ensdf/>
- [24] W. Zhang, B. Cederwall, Ö. Aktas, X. Liu, A. Erto-prak, A. Nyberg, K. Auranen, B. Alayed, H. Badran, H. Boston, et al., Observation of the proton emitter ¹¹⁶₅₇La₅₉, Communications Physics 5 (2022).
- [25] J. Erler, N. Birge, M. Kortelainen, W. Nazarewicz, E. Olsen, A. M. Perhac, M. Stoitsov, The Limits of the Nuclear Landscape, Nature (London) 486 (7404) (2012) 509–512.
- [26] M. Kortelainen, J. McDonnell, W. Nazarewicz, P.-G. Reinhard, J. Sarich, N. Schunck, M. V. Stoitsov, S. M. Wild, Nuclear Energy Density Optimization: Large Deformations, Phys. Rev. C 85 (2012) 024304. doi:10.1103/PhysRevC.85.024304. URL <https://link.aps.org/doi/10.1103/PhysRevC.85.024304>
- [27] P. Klüpfel, P.-G. Reinhard, T. J. Bürvenich, J. A. Maruhn, Variations on a theme by Skyrme: A systematic study of adjustments of model parameters, Phys. Rev. C 79 (2009) 034310. doi:10.1103/PhysRevC.79.034310. URL <https://link.aps.org/doi/10.1103/PhysRevC.79.034310>
- [28] G. Grams, W. Ryssens, G. Scamps, S. Goriely, N. Chamel, Skyrme-hartree-fock-bogoliubov mass models on a 3d mesh: Iii. from atomic nuclei to neutron stars, The European Physical Journal A 59 (11) (2023) 270.
- [29] V. Kejzlar, L. Neufcourt, W. Nazarewicz, P.-G. Reinhard, Statistical aspects of nuclear mass models, Journal of Physics G: Nuclear and Particle Physics 47 (9) (2020) 094001. doi:10.1088/1361-6471/ab907c. URL <https://dx.doi.org/10.1088/1361-6471/ab907c>
- [30] L. Neufcourt, Y. Cao, S. Giuliani, W. Nazarewicz, E. Olsen, O. B. Tarasov, Beyond the Proton Drip Line: Bayesian Analysis of Proton-Emitting Nuclei, Phys. Rev. C 101 (2020) 014319. doi:10.1103/PhysRevC.101.014319. URL <https://link.aps.org/doi/10.1103/PhysRevC.101.014319>

- [31] G. C. Ball, G. Hackman, R. Krücken, The triumph-isac facility: two decades of discovery with rare isotope beams, *Physica Scripta* 91 (9) (2016) 093002. doi:10.1088/0031-8949/91/9/093002. URL <https://dx.doi.org/10.1088/0031-8949/91/9/093002>
- [32] P. Bricault, R. Baartman, M. Dombbsky, A. Hurst, C. Mark, G. Stanford, P. Schmor, TRIUMF-ISAC Target Station and Mass Separator Commissioning, *Nuclear Physics A* 701 (1) (2002) 49–53, 5th International Conference on Radioactive Nuclear Beams. doi:[https://doi.org/10.1016/S0375-9474\(01\)01546-9](https://doi.org/10.1016/S0375-9474(01)01546-9). URL <https://www.sciencedirect.com/science/article/pii/S0375947401015469>
- [33] T. Brunner, M. Smith, M. Brodeur, S. Ettenauer, A. Gallant, V. Simon, A. Chaudhuri, A. Lapierre, E. Mané, R. Ringle, M. Simon, J. Vaz, P. Delheij, M. Good, M. Pearson, J. Dilling, TITAN’s digital RFQ ion beam cooler and buncher, operation and performance, *Nuclear Instruments and Methods in Physics Research Section A: Accelerators, Spectrometers, Detectors and Associated Equipment* 676 (2012) 32–43. doi:<https://doi.org/10.1016/j.nima.2012.02.004>. URL <https://www.sciencedirect.com/science/article/pii/S0168900212001398>
- [34] C. Jesch, T. Dickel, W. R. Plaß, D. Short, S. A. S. Andres, J. Dilling, H. Geissel, F. Greiner, J. Lang, K. G. Leach, W. Lippert, C. Scheidenberger, M. I. Yavor, The MR-TOF-MS isobar separator for the TITAN facility at TRIUMF, in: M. Wada, P. Schury, Y. Ichikawa (Eds.), *TCP 2014*, Springer International Publishing, Cham, 2017, pp. 175–184.
- [35] T. Dickel, S. A. S. Andrés, S. Beck, J. Bergmann, J. Dilling, F. Greiner, C. Hornung, A. Jacobs, G. Kripton-Koncz, A. Kwiatkowski, et al., Recent Upgrades of the Multiple-Reflection Time-of-Flight Mass Spectrometer at TITAN, *TRIUMF, Hyperfine Interactions* 240 (1) (2019) 1–9. URL https://link.springer.com/article/10.1007/978-3-319-1610-7_2
- [36] M. Reiter, S. A. S. Andrés, J. Bergmann, T. Dickel, J. Dilling, A. Jacobs, A. Kwiatkowski, W. Plaß, C. Scheidenberger, D. Short, C. Will, C. Babcock, E. Dunling, A. Finlay, C. Hornung, C. Jesch, R. Klawitter, B. Kootte, D. Lascar, E. Leistenschneider, T. Murböck, S. Paul, M. Yavor, Commissioning and Performance of TITAN’s Multiple-Reflection Time-of-Flight Mass-Spectrometer and Isobar Separator, *Nuclear Instruments and Methods in Physics Research Section A: Accelerators, Spectrometers, Detectors and Associated Equipment* 1018 (2021) 165823. doi:<https://doi.org/10.1016/j.nima.2021.165823>. URL <https://www.sciencedirect.com/science/article/pii/S0168900221008081>
- [37] T. Dickel, W. Plaß, A. Becker, U. Czok, H. Geissel, E. Haettner, C. Jesch, W. Kinsel, M. Petrick, C. Scheidenberger, et al., A high-performance multiple-reflection time-of-flight mass spectrometer and isobar separator for the research with exotic nuclei, *Nuclear Instruments and Methods in Physics Research Section A: Accelerators, Spectrometers, Detectors and Associated Equipment* 777 (2015) 172–188.
- [38] T. Dickel, W. Plaß, A. Becker, U. Czok, H. Geissel, E. Haettner, C. Jesch, W. Kinsel, M. Petrick, C. Scheidenberger, A. Simon, M. Yavor, A high-performance multiple-reflection time-of-flight mass spectrometer and isobar separator for the research with exotic nuclei, *Nuclear Instruments and Methods in Physics Research Section A: Accelerators, Spectrometers, Detectors and Associated Equipment* 777 (2015) 172–188. doi:<https://doi.org/10.1016/j.nima.2014.12.094>. URL <https://www.sciencedirect.com/science/article/pii/S0168900214015629>
- [39] T. Dickel, M. I. Yavor, J. Lang, W. R. Plaß, W. Lippert, H. Geissel, C. Scheidenberger, Dynamical time focus shift in multiple-reflection time-of-flight mass spectrometers, *International Journal of Mass Spectrometry* 412 (2017) 1–7. doi:<https://doi.org/10.1016/j.ijms.2016.11.005>. URL <https://www.sciencedirect.com/science/article/pii/S1387380616302664>
- [40] T. Dickel, W. R. Plaß, W. Lippert, J. Lang, M. I. Yavor, H. Geissel, C. Scheidenberger, Isobar Separation in a Multiple-Reflection Time-of-Flight Mass Spectrometer by Mass-Selective Re-Trapping, *Journal of The American Society for Mass Spectrometry* 28 (6) (2017) 1079–1090.
- [41] E. M. Lykiardopoulou, G. Audi, T. Dickel, W. J. Huang, D. Lunney, W. R. Plaß, M. P. Reiter, J. Dilling, A. A. Kwiatkowski, Exploring the limits of existence of proton-rich nuclei in the $z = 70 - 82$ region, *Phys. Rev. C* 107 (2023) 024311. doi:10.1103/PhysRevC.107.024311. URL <https://link.aps.org/doi/10.1103/PhysRevC.107.024311>
- [42] S. Ayet San Andrés, C. Hornung, J. Ebert, W. R. Plaß, T. Dickel, H. Geissel, C. Scheidenberger, J. Bergmann, F. Greiner, E. Haettner, C. Jesch, W. Lippert, I. Mardor, I. Miskun, Z. Patyk, S. Pietri, A. Pihktelev, S. Purushothaman, M. P. Reiter, A.-K. Rink, H. Weick, M. I. Yavor, S. Bagchi, V. Charviakova, P. Constantin, M. Diwisch, A. Finlay, S. Kaur, R. Knöbel, J. Lang, B. Mei, I. D. Moore, J.-H. Otto, I. Pohjalainen, A. Prochazka, C. Rappold, M. Takechi, Y. K. Tanaka, J. S. Winfield, X. Xu, High-resolution, accurate multiple-reflection time-of-flight mass spectrometry for short-lived, exotic nuclei of a few events in their ground and low-lying isomeric states, *Phys. Rev. C* 99 (2019) 064313. doi:10.1103/PhysRevC.99.064313. URL <https://link.aps.org/doi/10.1103/PhysRevC.99.064313>
- [43] S. Purushothaman, S. Ayet San Andrés, J. Bergmann, T. Dickel, J. Ebert, H. Geissel, C. Hornung, W. Plaß, C. Rappold, C. Scheidenberger, Y. Tanaka, M. Yavor, Hyper-EMG: A New Probability Distribution Function Composed of Exponentially Modified Gaussian Distributions to Analyze Asymmetric Peak Shapes in High-Resolution Time-of-Flight Mass Spectrometry, *International Journal of Mass Spectrometry* 421 (2017) 245 – 254. doi:<https://doi.org/10.1016/j.ijms.2017.07.014>. URL <http://www.sciencedirect.com/science/article/pii/S1387380616302913>
- [44] S. F. Paul, *emgfit 0.5.0* (2025). URL <https://pypi.org/project/emgfit/>
- [45] M. P. Reiter, S. Ayet San Andrés, E. Dunling, B. Kootte, E. Leistenschneider, C. Andreoiu, C. Babcock, B. R. Barquest, J. Bollig, T. Brunner, I. Dillmann, A. Finlay, G. Gwinner, L. Graham, J. D. Holt, C. Hornung, C. Jesch, R. Klawitter, Y. Lan, D. Lascar, J. E. McKay,

- S. F. Paul, R. Steinbrügge, R. Thompson, J. L. Tracy, M. E. Wieser, C. Will, T. Dickel, W. R. Plaß, C. Scheidenberger, A. A. Kwiatkowski, J. Dilling, Quenching of the $N = 32$ Neutron Shell Closure Studied via Precision Mass Measurements of Neutron-Rich Vanadium Isotopes, *Phys. Rev. C* 98 (2018) 024310. doi:10.1103/PhysRevC.98.024310.
URL <https://link.aps.org/doi/10.1103/PhysRevC.98.024310>
- [46] M. O. Kortelahti, K. S. Toth, K. S. Vierinen, J. M. Nitschke, P. A. Wilmarth, R. B. Firestone, R. M. Chasteler, A. A. Shihab-Eldin, Decay properties of ^{153}Yb and ^{153}Tm ; excitation energies of the $s_{1/2}$ and $h_{11/2}$ proton states in ^{153}Tm , *Phys. Rev. C* 39 (1989) 636–644. doi:10.1103/PhysRevC.39.636.
URL <https://link.aps.org/doi/10.1103/PhysRevC.39.636>
- [47] A. V. Potempa, V. P. Afanas'ev, Y. Vavryshchuk, h sub 11/2 and s sub 1/2 isomeric states in sup 155 tm. izomernye sostoyaniya h sub 11/2 i s sub 1/2 v sup 155 tm (May 1990).
- [48] B. Singh, Nuclear data sheets for $a = 151$, *Nuclear Data Sheets* 110 (1) (2009) 1–264. doi:<https://doi.org/10.1016/j.nds.2008.11.035>.
URL <https://www.sciencedirect.com/science/article/pii/S0090375208001300>
- [49] Martin, M.J., Adopted levels, gammas for ^{152}Sm , *Nucl. Data Sheets* 114 (2013) 1497.
- [50] C. Reich, Nuclear data sheets for $a = 154$, *Nuclear Data Sheets* 110 (10) (2009) 2257–2532. doi:<https://doi.org/10.1016/j.nds.2009.09.001>.
URL <https://www.sciencedirect.com/science/article/pii/S0090375209000805>
- [51] F. Kondev, M. Wang, W. Huang, S. Naimi, G. Audi, The NUBASE2020 evaluation of nuclear physics properties *, *Chinese Physics C* 45 (3) (2021) 030001. doi:10.1088/1674-1137/abddae.
URL <https://dx.doi.org/10.1088/1674-1137/abddae>
- [52] R. Broda, P. Daly, J. McNeill, R. Janssens, D. Radford, Level structure of $68\ 149\ \text{Er}\ 81$ and high-spin isomerism in proton-rich $N = 81, 82, 83$ nuclei, *Zeitschrift für Physik A Atomic Nuclei* 327 (1987) 403–408.
- [53] J. M. Nitschke, P. A. Wilmarth, J. Gilat, K. S. Toth, F. T. Avignone, Delayed proton emission of $N=81$ odd-odd precursors: ^{148}Ho , ^{150}Tm , and ^{152}Lu , *Phys. Rev. C* 37 (1988) 2694–2703. doi:10.1103/PhysRevC.37.2694.
URL <https://link.aps.org/doi/10.1103/PhysRevC.37.2694>
- [54] A. Potempa, K. Y. Gromov, J. Wawryszczuk, V. Kalinikov, Investigation of α -Decay of Spherical Nucleus Isomers with $Z > 64$, *Bulletin - Russian Academy of Sciences: Physics* 56 (1992) 666–666.
- [55] W. Huang, M. Wang, F. G. Kondev, G. Audi, S. Naimi, The AME 2020 Atomic Mass Evaluation (I). Evaluation of Input Data; and Adjustment Procedures, *Chinese Physics C: High Energy Physics and Nuclear Physics* 45 (3) (2021) – , 030002, 10.1088/1674-1137/abddb0.
- [56] C. Rauth, D. Ackermann, G. Audi, M. Block, A. Chaudhuri, S. Eliseev, F. Herfurth, F. Hessberger, S. Hofmann, H.-J. Kluge, et al., Direct mass measurements around $A = 146$ at SHIPTRAP, *The European Physical Journal Special Topics* 150 (2007) 329–335.
- [57] M. Block, D. Ackermann, K. Blaum, A. Chaudhuri, Z. Di, S. Eliseev, R. Ferrer, D. Habs, F. Herfurth, F. P. Heßberger, S. Hofmann, H. Kluge, G. Maero, A. Martín, G. Marx, M. Mazzocco, M. Mukherjee, J. B. Neumayr, W. R. Plaß, W. Quint, S. Rahaman, C. Rauth, D. Rodríguez, C. Scheidenberger, L. Schweikhard, P. G. Thirolf, G. Vorobjev, C. Weber, Mass measurements of exotic nuclides at SHIPTRAP, *AIP Conference Proceedings* 912 (1) (2007) 423–430. arXiv:https://pubs.aip.org/aip/acp/article-pdf/912/1/423/11695800/423_1_online.pdf, doi:10.1063/1.2746619.
URL <https://doi.org/10.1063/1.2746619>
- [58] K. S. Toth, Y. A. Ellis-Akovi, F. T. Avignone, R. S. Moore, D. M. Moltz, J. M. Nitschke, P. A. Wilmarth, P. K. Lemmertz, D. C. Sousa, A. L. Goodman, Single-Particle States in ^{149}Er and ^{149}Ho , and the Effect of the $Z=64$ Closure, *Phys. Rev. C* 32 (1985) 342–345. doi:10.1103/PhysRevC.32.342.
URL <https://link.aps.org/doi/10.1103/PhysRevC.32.342>
- [59] R. Broda, P. Daly, J. McNeill, R. Janssens, D. Radford, Level structure of $68\ 149\ \text{Er}\ 81$ and high-spin isomerism in proton-rich $n = 81, 82, 83$ nuclei, *Zeitschrift für Physik A Atomic Nuclei* 327 (1987) 403–408.
- [60] R. B. Firestone, J. M. Nitschke, P. A. Wilmarth, K. Vierinen, J. Gilat, K. S. Toth, Y. A. Akovi, Decay of $^{149}\text{Er}^{g+m}$ by Positron and Delayed Proton Emission and by Electron Capture, *Phys. Rev. C* 39 (1989) 219–232. doi:10.1103/PhysRevC.39.219.
URL <https://link.aps.org/doi/10.1103/PhysRevC.39.219>
- [61] M. Wang, W. Huang, F. Kondev, G. Audi, S. Naimi, The AME 2020 Atomic Mass Evaluation (II). Tables, Graphs and References, *Chinese Physics C* 45 (3) (2021) 030003. doi:10.1088/1674-1137/abddaf.
URL <https://doi.org/10.1088/1674-1137/abddaf>
- [62] M. Kortelainen, T. Lesinski, J. Moré, W. Nazarewicz, J. Sarich, N. Schunck, M. Stoitsov, S. Wild, Nuclear energy density optimization, *Physical Review C—Nuclear Physics* 82 (2) (2010) 024313.
- [63] S. Goriely, N. Chamel, J. Pearson, Further explorations of skyrme-hartree-fock-bogoliubov mass formulas. xii. stiffness and stability of neutron-star matter, *Physical Review C—Nuclear Physics* 82 (3) (2010) 035804.
- [64] J. Duflo, A. Zuker, Microscopic mass formulas, *Physical Review C* 52 (1) (1995) R23.
- [65] P. Möller, W. Myers, W. Swiatecki, J. Treiner, Nuclear mass formula with a finite-range droplet model and a folded-yukawa single-particle potential, *Atomic data and nuclear data tables* 39 (2) (1988) 225–233.
- [66] J. Dobaczewski, H. Flocard, J. Treiner, Hartree-fock-bogolyubov description of nuclei near the neutron-drip line, *Nuclear Physics A* 422 (1) (1984) 103–139.
- [67] J. Pearson, R. Nayak, S. Goriely, Nuclear mass formula with bogolyubov-enhanced shell-quenching: application to r-process, *Physics Letters B* 387 (3) (1996) 455–459.
- [68] C. Izzo, J. Bergmann, K. A. Dietrich, E. Dumlind, D. Fusco, A. Jacobs, B. Kootte, G. Kripkó-Koncz, Y. Lan, E. Leistenschneider, E. M. Lykiardopoulou, I. Mukul, S. F. Paul, M. P. Reiter, J. L. Tracy, C. Andreoiu, T. Brunner, T. Dickel, J. Dilling, I. Dillmann, G. Gwinner, D. Lascar, K. G. Leach, W. R. Plaß, C. Scheidenberger, M. E. Wieser, A. A. Kwiatkowski, Mass measurements of neutron-rich indium isotopes for

r-process studies, Phys. Rev. C 103 (2021) 025811. doi:
10.1103/PhysRevC.103.025811.

URL [https://link.aps.org/doi/10.1103/PhysRevC.
103.025811](https://link.aps.org/doi/10.1103/PhysRevC.103.025811)